

THERMOCAPILLARY-DRIVEN FLOW IN A FREE LIQUID FILM

Ichiro UENO

Department of Mechanical Engineering, Faculty Science & Technology
Tokyo University of Science
2641 Yamazaki, Noda, Chiba 278-8510, Japan
ich@rs.tus.ac.jp

Toshiki WATANABE

Division of Mechanical Engineering, School of Science & Technology
Tokyo University of Science
2641 Yamazaki, Noda, Chiba 278-8510, Japan
cattleya1232000@gmail.com

Takeshi KATSUTA

Division of Mechanical Engineering, School of Science & Technology
Tokyo University of Science
2641 Yamazaki, Noda, Chiba 278-8510, Japan
katsuta39@gmail.com

ABSTRACT

We focus on flow patterns in a free liquid film induced by thermocapillary effect, transition of the induced flow from a two-dimensional steady state to a chaotic state, and corresponding static/dynamic deformation of the film. The free liquid film is formed in a rectangular hole of $O(0.1 \text{ mm})$ in thickness under a designated temperature difference between the end walls. Temperature dependence of the surface tension results in a non-uniform surface tension distribution over the free surfaces, which leads unique flow patterns in the film. We employ a confocal laser displacement meter to detect the local positions in height of the free surfaces, and to detect the film thickness distribution under variable aspect ratio and volume ratio of the liquid film. We will introduce several flow patterns induced in the film and corresponding film profiles as functions of the aspect ratios and volume ratio of the film. Under unity volume ratio to the volume of the hole to suspend the liquid film, we have two major basic flow patterns at small-enough thermocapillary effect; double-layered basic flow and single-layered basic flow. The net flow direction of the fluid in both cases is from hot- to cold-end walls. In the case of volume ratio of the film is larger than unity, it is found that the net flow direction becomes opposite to the normal case. We will discuss the occurring condition of those flow patterns and the effect of the shape of the film against those patterns.

INTRODUCTION

Understanding and controlling of heat and mass transfers in a fluid in micrometer scale has been more indispensable

than ever for developing micrometer-scale reactors and actuators in recent years. It has been a common knowledge that we must face a significant pressure loss in such micrometer-scale fluid devices, so that we must prepare a rather large pressure difference to drive the fluid in the system. Driving fluid by surface-tension difference is a potential way to overcome those problem because effect of surface forces on the system becomes more dominant than that of volume forces as the scale of the system decreases. If one has a free surface in the system and the fluid has a non-zero temperature and/or concentration coefficient of surface tension, one can drive the fluid by adding a temperature/concentration difference over the free surface. As for driving a fluid by use of the temperature dependence of the surface tension, that is, the thermocapillary effect, there exist researches aiming fine controls of liquid migration (Darhuber et al., 2003), pumping effect (Sammarco & Burns, 1999), and so on. One must understand the fundamental dynamics of the free-surface-driven fluid flow in a thin liquid film exposed to a temperature difference or temperature gradient along the free surface for those system.

One realizes time-dependent 'oscillatory' flow in the film if one puts a larger temperature difference to the liquid film. In the case of thin liquid film formed in an open cavity (the film with a single free surface), we have an instability known as a hydrothermal wave (HW, hereafter) instability. Smith & Davis (1983) performed a linear stability analysis on a thermocapillary flow in an infinite thin liquid layer imposed by a constant temperature gradient along a free surface. They predicted a new instability in which oblique temperature

waves travel over the liquid film with an angle inclined to the mean temperature gradient. Riley & Neitzel (1998) and Kawamura et al. (2007) experimentally proved the existence of the HW afterward.

In the case of the free liquid film with two free surfaces, on the other hand, we have little knowledge on the flow patterns and transition processes in the film exposed to a temperature difference between the both end walls. It is noticed that Dr. Donald Pettit, an American astronaut, exhibited a unique demonstration on fluid flow and phase change in a thin free liquid film that has two free surfaces sustained in a closed ring (see Fig. 1) in the International Space Station (ISS) in 2003 (Phillips, 2003). One can form a free liquid film of even O(100 mm) in diameter under microgravity condition, because the surface tension and wettability are dominant as in the micrometer-scale system. Free liquid film brings us a vigorous advantage; there exists less wall friction due to a contact with the solid wall comparing to systems of liquid film in a cavity sustained by the bottom wall as well as side wall. That means one need less energy to drive the fluid in the film than in the liquid film sustained in a cavity, that is, the liquid film with a single free surface. With a small temperature difference, time-independent steady flows appear in the film. Ueno & Torii (2010) has indicated a HW-like instability in which a series of oblique thermal waves propagate from the colder end toward the hotter end by three-dimensional numerical simulation. We have little information, however, on ‘oscillatory’ flows in the free liquid films. In the present paper, we especially focus on flow patterns in a free liquid film induced by the thermocapillary effect and transition of the induced flow from a two-dimensional steady state to a chaotic state. We also focus on the correlation between the oscillatory flows and the dynamic deformation of the liquid film.

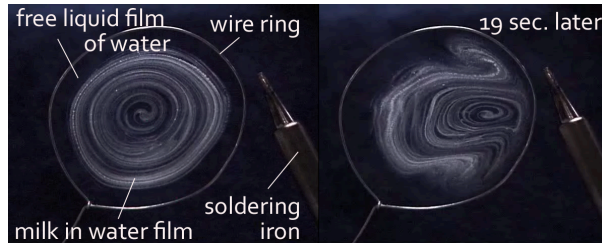


Figure 1. Demonstration of surface-tension-difference-driven flow in a free liquid film carried out by Dr. Donald Pettit, an American astronaut in the International Space Station (ISS) (© NASA)

EXPERIMENT

Target geometry is schematically shown in Fig. 2. A free liquid film of 5-cSt silicone oil is formed in a hole in an aluminum plate. Dimension of the hole is described with L_x , L_z and d for streamwise length, spanwise length (width), and depth, respectively. Shape of the hole is described with aspect ratios of $\Gamma_x = L_z/L_x$ and $\Gamma_y = L_x/d$. The film is sustained by its surface tension and wettability. The volume of the liquid film is described by the volume ratio V/V_0 , where V is the volume

of the liquid concerned, and V_0 the volume of the hole region ($= L_x L_z d$). The film is exposed to a designated temperature difference, $\Delta T = T_h - T_c$, between the end walls of the hole. Intensity of the thermocapillary effect imposed to the film is described by non-dimensional Marangoni number $Ma = |\sigma_T| (\Delta T/L_x) d^2 / (\rho \nu \kappa)$, where σ_T is the temperature coefficient of the surface tension, ρ the density, ν the kinematic viscosity, and κ the thermal diffusivity. The physical properties of the test fluid are listed in Table 1.

The flow is visualized by suspending gold-coated acrylic sphere particles of 30 μm in diameter and of 1770 kg/m^3 in density, and observed by a CCD camera. The surface temperature is measured by an infrared camera. The local positions of the top and bottom surfaces of the film are scanned by a confocal displacement sensor. It is noted here that the fluid flows induced in the liquid film are dominant by the thermocapillary effect; the dynamic Bond number Bo_D is of $O(10^{-1})$ in the case of $d = 0.6$ mm, and of $O(10^{-3})$ in the case of $d = 0.2$ mm.

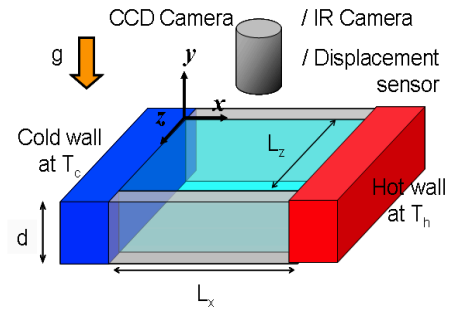


Figure 2. Target geometry; a free liquid film exposed to a temperature difference ΔT .

Table 1. Physical properties of the test fluid (silicone oil of 5 cSt at 25°C) (Shin’etsu Chem. 1991)

density, ρ [kg/m^3]	kinematic viscosity, ν [m^2/s]	thermal diffusivity, κ [m^2/s]	surface tension, σ [N/m]	temp. coeff. of σ , $ \sigma_T $ [N/m K]
9.15×10^2	5.0×10^{-6}	7.31×10^{-8}	1.97×10^{-2}	6.37×10^{-5}

RESULTS & DISCUSSION

We have two kinds of steady flows under the small ΔT ; that is, the double-layered basic flow and the single-layered basic flow. Typical examples of the induced double-layered and the single-layered flows in the liquid film of $V/V_0 \sim 1.0$ are shown in Figs. 3 and 4, respectively. Those figures consist of the path line (left), the top surface temperature (center), and the positions of free surfaces and the thickness distribution along the center line of the film (right above and below, respectively). The path line is obtained by exposing for 1.0 s. In the case of rather thick liquid film, the double-layered basic flow emerges as shown in Fig. 3; that is, the fluid flows from

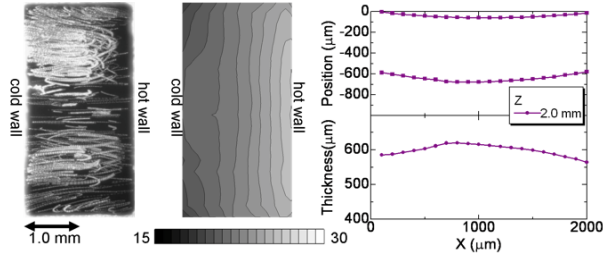


Figure 3. Typical example of the induced flow in the film of $V/V_0 \sim 1.0$; the path line for 1.0 s (left), the top surface temperature (center) observed with IR camera, and the positions of free surfaces and the thickness distribution along the center line of the film (right) in the case of $(L_x, L_z, d) = (2.0, 4.0, 0.6)$ [mm] at $\Delta T = 15.0$ [K].

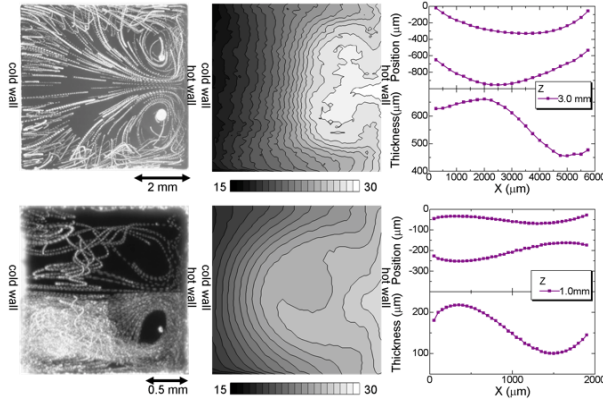


Figure 4. Typical examples of the induced flow in the film of $V/V_0 \sim 1.0$ in the volume ratio in the case of $(L_x, L_z, d) = (6.0, 6.0, 0.6)$ [mm] (top frames) and $(2.0, 2.0, 0.2)$ [mm] (bottom) at $\Delta T = 15.0$ [K]. Each frame indicates the same as in Fig. 3.

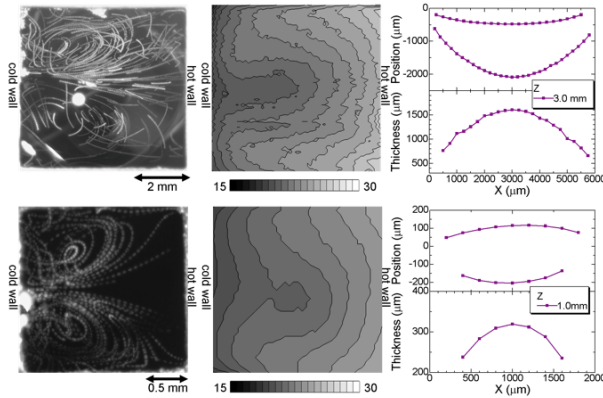


Figure 5. Typical example of the induced flow in the film of $V/V_0 > 1.0$; other conditions are the same as indicated in Figs. 3 & 4. One can clearly see the fluid flow from the cold-end to the hot-end walls at the center of the film.

the hot-end wall to the cold-end wall on the top and bottom surfaces of the film, and returns inside the film toward the hot-end wall. Isothermal lines over the top free surface lie in the direction almost perpendicular to the net temperature gradient, or almost parallel to the end walls. Under this condition, both free surfaces are convex downward, in the almost same manner for the top and the bottom. That is, the film sags a bit under its own weight in spite of the convective motion of the fluid. The dynamic Bond number in this case is of 0.16. Profile of the film thickness, on the other hand, reflects the flow pattern induced in the film; the both ends are fixed to the end walls, and the thickest part is located slightly downstream from the center due to the thermocapillary flow toward the cold-end wall.

In the rather thin case, on the other hand, a single-layered span-wise cellular pattern emerges in the film; that is, the fluid flows from the hot-end wall to the cold at the center of the film, and returns along the side walls. This flow pattern consists of a pair of vortices located in the spanwise direction. This is a unique convective behavior comparing to a system of a thin liquid film with a single free surface. Figure 4 indicates typical examples of the single-layered flow in the liquid films of the same aspect ratio but of different depth. For both cases the center of the vortices are located near the hot-end wall. And hotter fluid heated by the hot-end wall flows into the center part of the film, and the colder fluid cooled by the cold-end wall returns along the side walls. The positions of the top/bottom free surfaces at the center of the film are completely different between the thicker and thinner films. In the thicker film case, the film sags under its own weight due to the gravity. In the thinner case, on the other hand, the effect of the gravity becomes weak enough to realize symmetrically deformed liquid film. That is, the positions of the top and bottom surfaces are almost symmetric to the center line of the film. Noted that profiles of the film thickness are almost similar for both cases. The convective motion of the fluid leads the convex at the downstream region of the film, and the concave at the upstream region.

What we pay our attention to is the volume ratio of the liquid film in the case of single-layered steady flow. We vary the volume ratio of our liquid film aforementioned in order to make sure the effect of the volume ratio of the film concerned. Typical examples of the induced flow in the convex film ($V/V_0 > 1.0$) are shown in Fig. 5. It is obvious that the centers of the vortices are located near the cold-end wall, and the colder fluid cooled at the cold-end wall is brought toward the hot-end wall. These aspects are opposite to the features described in Fig. 3. It is found that one can control the net flow direction in a thin free liquid film by varying its volume; a ‘reverse flow’ is realized in the liquid film of $V/V_0 > 1.0$. Such an occurrence of the ‘reverse flow’ can be explained by considering a temporal development of the thermal field at an early stage of the experiment. When a temperature difference is added between the both end walls, the heat diffuses in the liquid film toward the cold-end wall. Area through which the heat passes is significantly varied when the volume ratio of the liquid film is changed. In the case of $V/V_0 \sim 1.0$, the heat diffuses in the film of the same area. So that the surface temperature develops almost parallel to the end wall. The fluid is supposed to flow toward the cold-end wall against the friction near the

side wall, so the fluid easily flows in the middle part of the film in the spanwise direction. In the case of fat liquid film of $V/V_0 > 1.0$, on the other hand, the heat diffuses in the convex film whose area at the middle is the largest. So that the surface temperature develops faster near the side walls comparing to the middle part. Such a non-uniform development of the thermal field leads the fluid preferably flow along the side walls first, which results in the ‘reverse flow.’

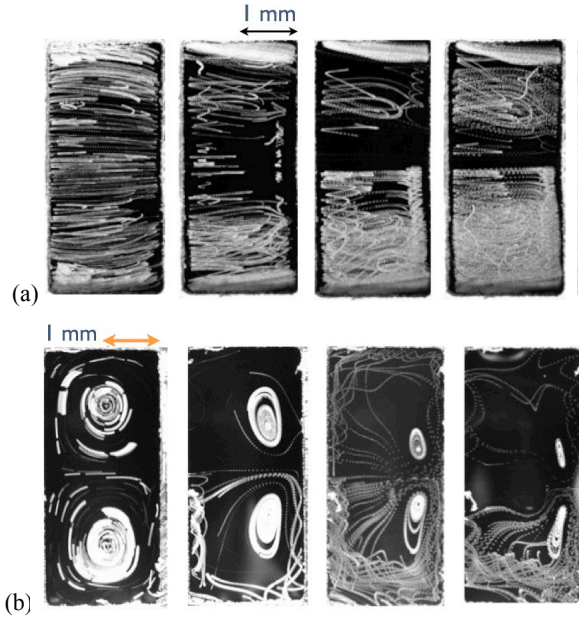


Figure 6. Typical examples of the induced flow in the film of $V/V_0 \sim 1.0$ and of (L_x, L_z, d) [mm] = (a) (2.0, 4.0, 1.2) and (b) (2.0, 4.0, 0.2) observed from above; (a) $\Delta T = 2.3$ K ($Ma = 3.1 \times 10^2$), 25.3 K (3.5×10^3), 40.1 K (7.4×10^3) and 46.5 K (9.2×10^3) and (b) $\Delta T = 0.6$ K ($Ma = 2$), 5.5 K (20), 12.8 K (48) and 17.0 K (70) from left to right.

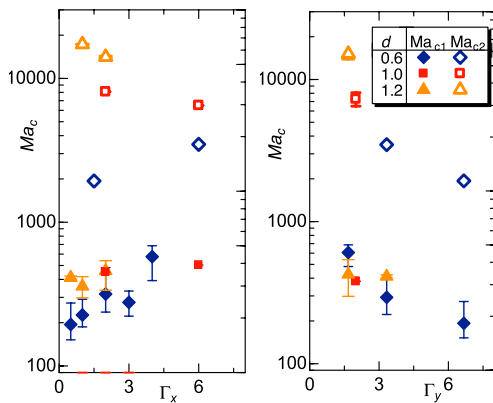


Figure 7. Onsets of 1st (from steady to inner oscillation) and 2nd (from inner to fully 3D oscillations) transitions as functions of (a) aspect ratio Γ_x and (b) Γ_y .

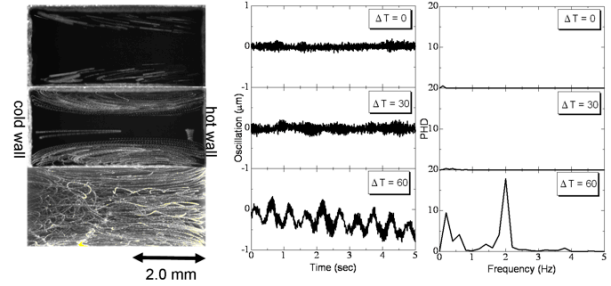


Figure 8. Example of the induced flow; the path line observed from above the film (left) the top surface oscillation (middle) and its spectra (right) observed from above in the case of (L_x, L_z, d) [mm] = (4.0, 2.0, 1.2) and $\Delta T = 0, 30$ and 60 [K]. The path line is obtained by integrating frames for 5.0 s.

As increasing Ma , the flow in the film becomes time-dependent ‘oscillatory’ flow as shown in Fig. 6 (a) and (b) for double-layered and single-layered flows, respectively. Here we focus on dynamic surface deformation in time-dependent ‘oscillatory’ flow in the double-layered-flow case. In such flow patterns, one can realize a hydrothermal-wave-like instability in the film (Ueno & Torii, 2010). Figure 7 indicates the occurring conditions of the oscillatory flow against the aspect ratios. After the onset of the oscillation, the liquid film exhibits dynamic deformation according to the time-dependent flow. Figure 7 indicates examples of temporal variations of the top surface position at the center of the film (left) and its power spectra (right) under various ΔT . After the onset of the oscillation, the film exhibits a dynamic motion with a fundamental frequency. In the present range of the experiments, the dynamic deformation of the liquid film is perfectly synchronized with the time-dependent flow; the fundamental frequency of the dynamic deformation corresponds to that of the temporal variation of the surface temperature measured by IR camera (Ueno & Torii 2010). We will present occurring conditions of the flow patterns and their routes to the chaotic flows.

CONCLUDING REMARKS

Thermocapillary-driven flow induced in a free thin liquid film under a temperature gradient parallel to the free surfaces is investigated by experimental approach. A double-layered basic flow appears under a small thermocapillary effect as the prediction by the simulation by Ueno & Torii (2010). One has two transitions of the flow field in the liquid film by increasing a temperature gradient. That is, ‘‘internal’’ oscillatory flow and fully oscillatory flow. In the case of thinner liquid film, single-layered basic flow is emerged. No one can find any double-layered structure in the film, but the single-layered span-wise cellular pattern. The authors indicate a critical Marangoni number by Ma and aspect ratio Γ_y for the double-layered flow.

Flow patterns and corresponding static/dynamic deformation in a thin free liquid film induced by thermocapillary effect is discussed. We firstly evaluate the

positions of the top and bottom surfaces and thickness distribution of the film in the case of the steady double-layered and single-layered basic flows. We then focus on the effect of the volume ratio of the liquid film on the induced flow pattern. Qualitative explanation is made on a unique flow pattern, in which the net flow direction is from the cold-end wall to the hot-end wall, demonstrated by Dr. Donald Pettit aboard the International Space Station (Phillips, 2003). Finally we detect the dynamic surface deformation due to the thermocapillary effect after the onset of the time-dependent 'oscillatory' flow.

ACKNOWLEDGEMENTS

We acknowledge Research Institutes of Science & Technology (RIST), Tokyo University of Science, for their supports to carry out a series of experiments.

REFERENCES

- Darhuber, A. A., Davis, J. M., Troian, S. M. & Reisner, W. W., 2003, Thermocapillary actuation of liquid flow on chemically patterned surfaces, *Phys. Fluids* 15, pp.1295-1304.
- Kawamura, H., Tagaya, E., Hoshino, Y., 2007, A consideration on the relation between the oscillatory thermocapillary flow in a liquid bridge and the hydrothermal wave in a thin liquid layer, *Int. J. Heat Mass Trans.* 50. pp. 1263-1268.
- Phillips, T., 2003, Saturday Morning Science, Feb. 25, 2003, from http://science.nasa.gov/headlines/y2003/25feb_nosoap.htm
- Riley, R. J. & Neitzel, G. P., 1998, Instability of thermocapillary-buoyancy convection in shallow layers. Part 1. Characterization of steady and oscillatory instabilities, *J. Fluid Mech.* 359, pp.143-164.
- Sammarco, T. S. & Burns, M. A., 1999, Thermocapillary pumping of discrete drops in microfabricated analysis devices, *AIChE Journal* 45, pp.350-366.
- Shin-Etsu Chemical Co., Ltd., 1991, *Technical note - silicone oil KF96*. (in Japanese).
- Smith, M. K. & Davis, S. H., 1983, Instabilities of dynamic thermocapillary liquid layers. Part 1. Convective instabilities, *J. Fluid Mech.* 132, pp.119-144.
- Ueno, I. & Torii, T., 2010, Thermocapillary-driven flow in a thin liquid film sustained in a rectangular hole with temperature gradient. *Acta Astronautica* 66, pp.1017-1021.